Article

Not peer-reviewed version

# Synthesis under normal conditions, morphology and composition of $AlF_3$ nanowires

Albert Dautov *, Konstantin Kotlyar, Denis Butusov, Ivan Novikov, Aliya Khafizova, Artur Karimov

Posted Date: 7 August 2023

doi: 10.20944/preprints202308.0485.v1

Keywords: AlF3 nanowires; hydrofluoric acid; metal fluorides

*Article*

# Synthesis under Normal Conditions, Morphology and Composition of $AlF_3$ Nanowires

**Albert Dautov [1,2,*], Kotstantin P. Kotlyar [2,3,4], Deins Butusov [5], Ivan Novikov [1], Aliya Khafizova [1] and Artur Karimov [6]**

1 Faculty of Electronics, St. Petersburg State Electrotechnical University "LETI" 197376 St. Petersburg, Russia
2 Faculty of Physics, St. Petersburg State University, Universitetskaya Embankment 13B,199034 St. Petersburg, Russia
3 Department of Physics, Alferov University, Khlopina 8/3, 194021 St. Petersburg, Russia
4 Institute for Analytical Instrumentation RAS, Rizhsky 26, 190103 St. Petersburg, Russia
5 Youth Research Institute, St. Petersburg Electrotechnical University "LETI", 5 Professora Popova St.,197376 Saint Petersburg, Russia
6 Computer-Aided Design Department, St. Petersburg Electrotechnical University "LETI",5 Professora Popova St., 197376 Saint Petersburg, Russia
* Correspondence: amdautov24@gmail.com

**Abstract:** $AlF_3$ has interesting electrophysical properties, due to which the material is promising for applications in supercapacitors, UV coatings with low refractive index, excimer laser mirrors, and photolithography. The formation of $AlF_3$-based nano- and micro-wires can bring new functionalities to $AlF_3$ material. $AlF_3$ nanowires be used, for example, in functionally modified microprobes for scanning probe microscopy. In this work, we investigate the $AlF_3$ samples obtained by the reaction of initial aluminum with aqueous hydrofluoric acid solution of different concentrations. All the samples were obtained under normal conditions. The morphology of the nanowire samples is studied by scanning electron microscopy. Quantitative energy-dispersive x-ray spectroscopy (EDS) spectra are obtained and analyzed with respect to the feedstock and each other.

**Keywords:** $AlF_3$ nanowires; hydrofluoric acid; metal fluorides

## 1. Introduction

Metal fluorides are promising for applications in catalysis [1-6], as ionic conductors [7] and luminescent materials [8-11]. One of the most important representatives of these binary compounds is aluminum fluoride ($AlF_3$), which is an inorganic crystalline substance under normal conditions. Due to its electrophysical properties, it finds application as a catalyst in organic synthesis, an additive for electrolyte to lower the melting point, fluxes for oxide separation and removal [12], an element of multilayer optical structures [13], a material for fabrication of far-infrared mirrors [14]. It is also a promising candidate for fiber lasers in the mid-infrared region [15]. $AlF_3$/polyimide films increase dielectric permeability as well as reduce leakage currents compared to conventional polyimide films [16]. Interestingly, AlF3 can also be used to prevent tooth discoloration [17]. $AlF_3$ can be used as a film to cover lithium-sulfur batteries to prevent the "shuttle effect" that causes a rapid decrease in capacity [18]. Synthesis of $AlF_3$ in the form of one-dimensional (1D) structures, such as nanorods, nanowires (NWs) and nanotubes, enables a high surface to volume ratio. This makes 1D $AlF_3$-based structures promising for use in supercapacitors and nano-probes of different types [19-23]. There are several methods for producing 1D structures, including $AlF_3$-based NWs [24-30], each characterized by a complicated technological process. Particularly, it is difficult to obtain $AlF_3$ without the use of aggressive HF. One of the most popular methods for synthesizing $AlF_3$ nanoparticles is the fluorolitic sol-gel synthesis [31], which can be described by the system of equations

$$\text{M-OR} + \text{H-F} \rightarrow \text{M-F+ROH} \quad (1)$$

$$nM\text{-}F \rightarrow (\text{-}N\text{-}F\text{-}M\text{-}F)n/2 \quad (2)$$

In the first reaction, the water as a reactant is completely replaced with hydrogen fluoride, which leads to the formation of M-F bonds. The second reaction, if performed correctly, leads to the formation of either metal oxides or nanoscale metal fluorides. Fluoride ions tend to form stable bonds. Consequently, there are not many examples of crystalline fluorides containing fluorine at the ends. The main problem in the synthesis of metal fluorides is their high lattice energy, which makes it difficult to form regular crystal structures [32]. On top of that, the existing technological methods require relatively high temperatures (450-500°C), as well as additional raw materials for the intermediate reactions. Thus, the development of simple and robust methods to synthesize $AlF_3$ NWs is a challenging task.

This paper presents the synthesis method and the results of morphological and compositional characterization of $AlF_3$ NWs. The NWs are obtained in the direct reaction of hydrofluoric acid solution with aluminum under normal conditions. The morphology and composition of the NW samples are studied versus the concentrations of hydrofluoric acid reacting with pure aluminum.

## 2. Materials and methods

The growth experiments were carried out as follows. A sample of mass m=2.435 g was placed in a 70 ml volume of hydrofluoric acid in a polypropylene vessel. At the beginning, the entire area of the sample was covered with a white film, and bubbles gradually began to appear in the volume. Twenty-five minutes later, the reaction transitioned to the active stage, with fast outgassing. Two hours later, the sample dissolved completely. The solution was left to await precipitation. Twenty-four hours later, a crystal formed, which was treated with 2-methanol propane to prevent contact with the solution residue.

The morphology and composition of the original aluminum and synthesized samples were studied using a scanning electron microscope (SEM) Zeiss Supra25 (Carl Zeiss), equipped with an energy dispersive x-ray analyzer (EDX) Ultim Max 100 (Oxford Instruments). Aluminum used for the production of 1.7-liter pots by KALITVA COOK was a raw material for the study ($Al_f$). In the analysis of the alloy by EDX method, the following composition was determined: Al=98.95%, Si=0.67%, Ca=0.05%, Fe=0.21%, Ni=0.13%, and Zn - 0.02%. Granulated pure Al ($Al_p$) was also used, with an average pellet mass of m=0.246g. Hydrofluoric acid from "Sigma Tech" was used as an oxidizer. NT-MDT NTEGRA THERMA was used for atomic force microscopy (AFM) analysis.

The crystal is transparent, has a characteristic odor, and resembles table salt crystals in brittleness. A series of experiments with different concentrations of hydrofluoric acid were performed, with the volume of the solution always kept at 40 ml. For all samples a precipitate in the solution after the formation of crystals was observed. Table 1 shows the acid concentrations and the ratio of the mass of the initial metal over the mass of the precipitate. Comments referring to these samples are given later in the text. In addition, a similar series of experiments with $Al_f$ was performed.

**Table 1.** Data from the tested samples of $Al_f$.

| Sample | percentage of solution concentration, % | $\frac{m(residue)}{m(Al_f)}, g$ |
|---|---|---|
| 1.1 | 40 | 12.49 |
| 2.1 | 32.6 | 10.67 |
| 3.1 | 29.4 | 9.77 |
| 4.1 | 24.5 | 11.34 |
| 5.1 | 16.3 | 10.12 |
| 6.1 | 8 | 14.32 |

Preprints (www.preprints.org) | NOT PEER-REVIEWED | Posted: 7 August 2023 doi:10.20944/preprints202308.0485.v1



## 3. Results and discussion

In the first experiment it was assumed that $AlF_3{\cdot}H_2O$ was obtained. A known method of obtaining aluminum fluoride by neutralizing hydrofluoric acid with aluminum hydroxide $3HF+AL(OH)_3=AlF_3+3H_2O$ at 90-95 °C for one hour. During the reaction, aluminum fluoride crystallizes as $AlF_3{\cdot}H_2O$, after which the paste is dehydrated at 350°C [33]. It is possible that the additives in the original food-grade aluminum alloy served as a catalyst for the reaction. However, this reasoning was not confirmed by a series of tests with $Al_f$ pellets.

According to the AFM results obtained, exposure to HF disturbed the integrity of the original surface, forming a stepped-grid structure. As can be seen, the flaking of the structure occurred uniformly, regardless of variations in the height of the original relief. Based on the assumption that the destruction of the sample material occurred under the catalytic effect of a certain alloy constituent, we can conclude that its greatest concentration was in the places under the "steps" where dissolution was the most intense. A series of tests with hydrofluoric acid of different concentrations was also carried out.

As the concentration of hydrofluoric acid in the solution increased, the initial structure of the resulting precipitate changed. During the reaction of sample 6.1 with 8% solution, the precipitate obtained during the reaction copied the shape of the container in which the experiment took place in Figure 1 (b). The sample has a sandwich structure: a transparent layer in the middle and a white salt-like surface. In the experiment with sample 1.1, the precipitate did not form a structure but fell out as flakes. In addition to the precipitate, a thin layer of unreacted Al remained in the container. It is interesting that samples 1.1-1.2 turned out to be unstable and after two weeks acquired a macro-porous structure, as shown in Figure 1 (a).

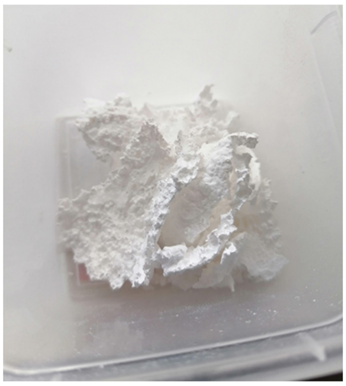

(**a**)

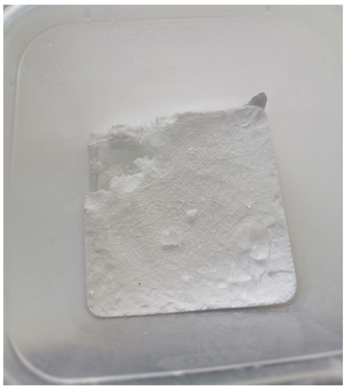

(**b**)

**Figure 1.** Samples obtained with different solution concentrations: (**a**) 32.6; (**b**) 8%.

The chemical composition of the obtained samples was investigated using EDX, while SEM visualization represented the morphology of the output structures. Figure 2 shows a comparative analysis of the spectra of the initial aluminum and the studied substance. According to the peaks, we can conclude that the resulting material consists mainly of Al and F. The calculated atomic percentages of different elements are the following: F =71.17%; Al =29.53%; Si =0.57%; Fe =0.08%; Ni =0.08%, and Zn=0.01%. Figure 3 shows the images obtained by scanning SEM in the analysis of sample 6.1.

Preprints (www.preprints.org) | NOT PEER-REVIEWED | Posted: 7 August 2023 doi:10.20944/preprints202308.0485.v1



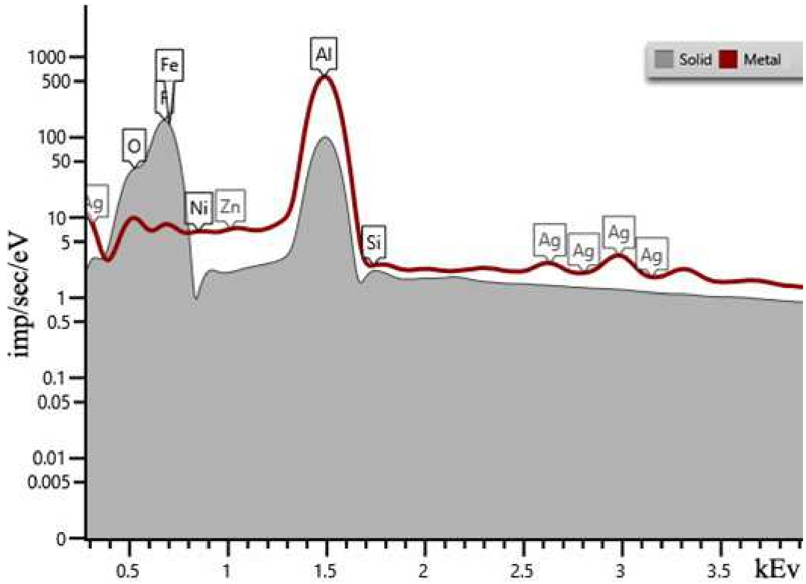


**Figure 2.** EDX spectra of sample 6.1 ("solid"). "Metal" represents Alf.

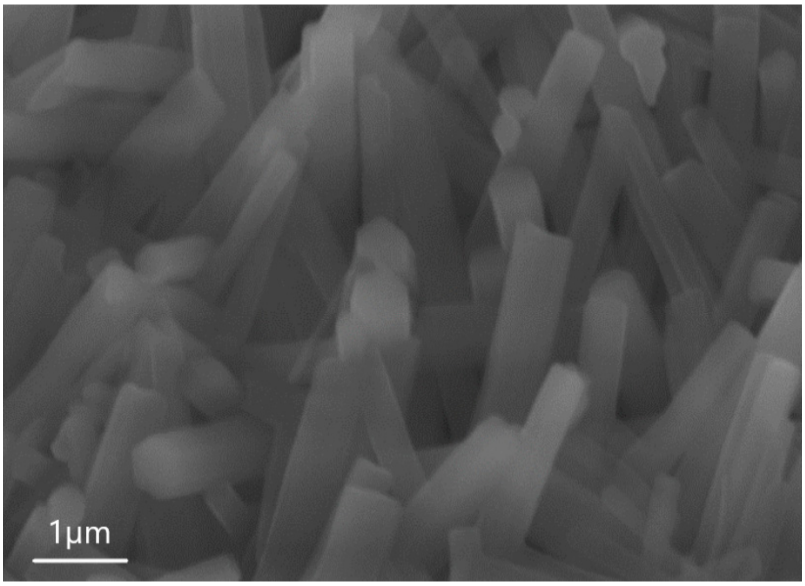


**Figure 3.** SEM image of sample 6.1, showing that the structure consists of $AlF_3$ microwires of ~ 1 m width.

Figure 3 shows that the surface consists of an ensemble of 1D microwires. The average height of 1D structures is 4 μm, the length of the hexagon side is 0.82 μm, and the surface density is in the order of $10^4$ 1/cm$^2$. EDX was also used to determine the composition. The analysis revealed that the percentage of Zn in the microwires was higher than in the matrix as a whole. It is interesting that, depending on the concentration of the solution with which the starting material interacted, the size of the wires and their geometry change. For example, Figure 4 shows an SEM image of sample 5.1, where the NWs are thinner than in sample 6.1.

 doi:10.20944/preprints202308.0485.v1



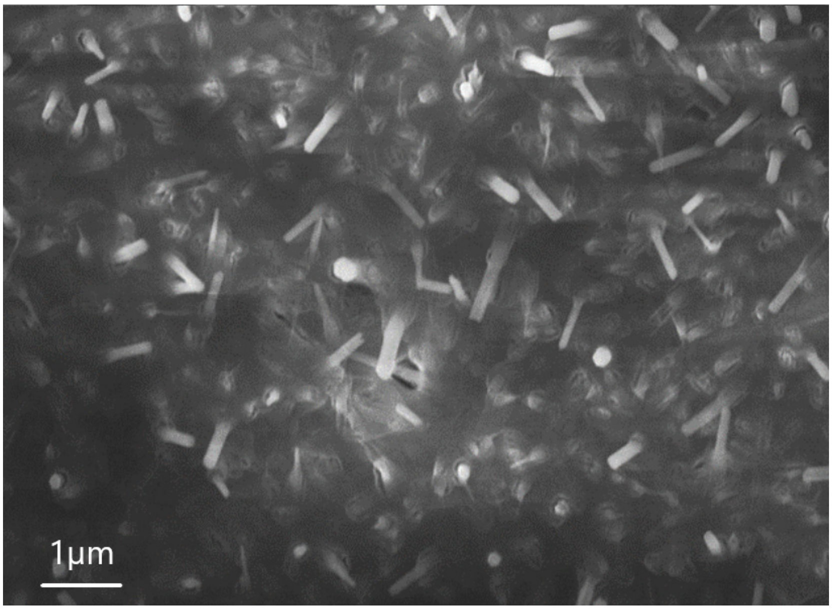


**Figure 4.** SEM image of sample 5.1.

The average height of these NWs is 1 μm, the length of the hexagon side is 0.26 μm, and the surface density is in the order of $3 \cdot 10^4$ 1/cm². Under normal conditions, the thermodynamically stable $\alpha$-$AlF_3$ phase is a rhombic structure similar to that of perovskite. The β-$AlF_3$ rhombic phase has a hexagonal structure [34]. β-$AlF_3$ is synthesized by two methods: by dehydration of $\alpha$-$AlF_3 \cdot 3H_2O$ and by growing crystals from chloride flux [14]. There are other metastable phases of $AlF_3$ (tetragonal and cubic), whose structures are little studied. When analyzing the structures using SEM, a tendency of charging of the samples was observed. From the first sample to the sixth, the charging capacity of the sample increased, due to which the obtained images had a noise background.

SEM of sample 4.1 revealed that the NWs have a nearly perfect cylindrical shape (Figure 5), and that overall pattern of the NWs resembles a herringbone branch. The average height of these NWs is 4 μm, the average diameter is around 0.4 μm; and the surface density is in the order of $4 \cdot 10^4$ 1/cm². During the study of the formation of 1D structures, an interesting fact was discovered - NWs did not form in all reactions. In the synthesis of sample 1.1, no NWs were formed, and the microstructure of the material is a rough surface.

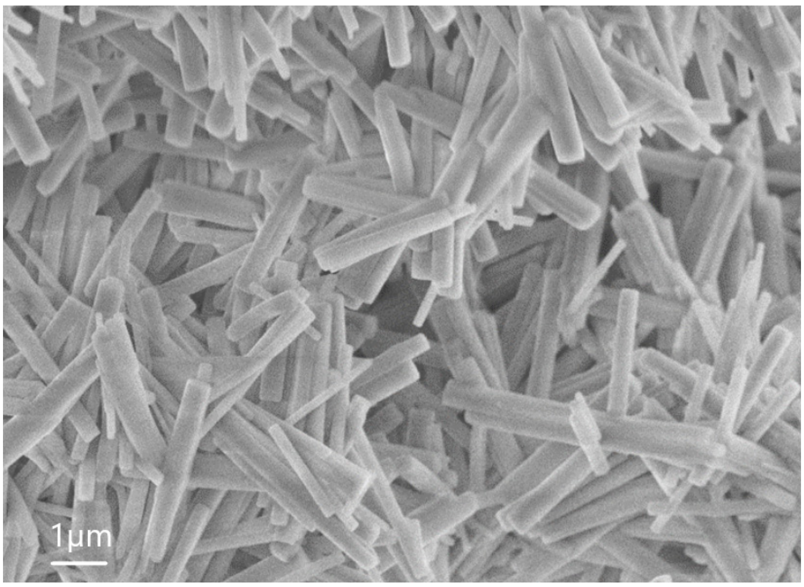


**Figure 5.** SEM image of sample 4.1.

Preprints (www.preprints.org) | NOT PEER-REVIEWED | Posted: 7 August 2023 doi:10.20944/preprints202308.0485.v1



For a clearer result, we performed a series of experiments with particularly pure Al ($Al_P$). Table 2 presents the experimental data (in the synthesis of sample 5.2 the mass of the initial aluminum was lower than average, which may have affected the overall dependence of the given ratios). Figure 6 shows the SEM images of the obtained samples. The data of the $Al_f$ and $Al_P$ reactions appear very similar.

**Table 2.** Data from the tested samples of $Al_P$.

| Sample | percentage of solution concentration, % | $\frac{m(residue)}{m(Al_p)}$ |
|---|---|---|
| 1.2 | 40 | 120.65 |
| 2.2 | 32.6 | 93.31 |
| 3.2 | 29.4 | 81.04 |
| 4.2 | 24.5 | 53.81 |
| 5.2 | 16.3 | 115.37 |

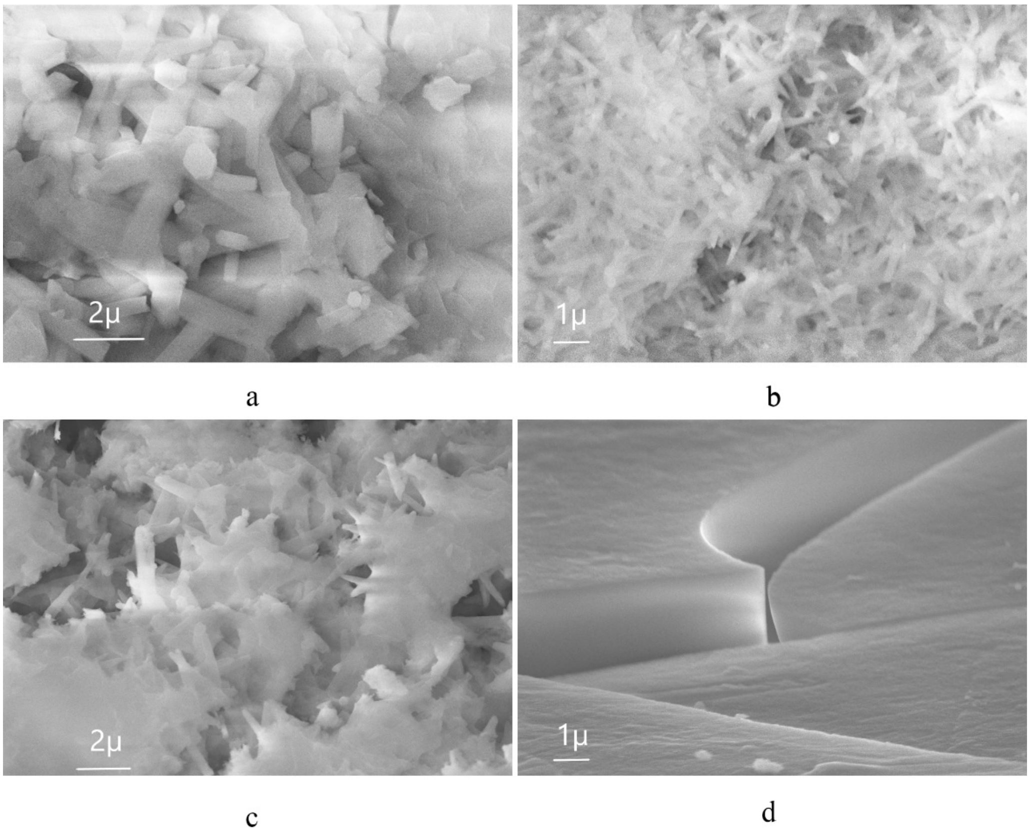


**Figure 6.** SEM image of the resulting $AlF_3$ based on $Al_P$, differing in solution concentration: (**a**) 8%; (**b**) 16.3%; (**c**) 32.6%; (**d**) 40%.

The sample in Figure 6 (**a**) was obtained during the reaction of $Al_P$ with 8% solution. The geometry of 1D structures is similar to that shown in Figure 4. According to the SEM data, we can also say that the obtained samples exhibit the ability to accumulate charge. We clearly observe a structural transformation of the surface, from a completely smooth surface with the presence of local dislocations to a complete coverage of the surface with NWs.

The difference is also observed in the macrostructure. In the 8% solution, the sample is completely white without the formation of an additional phase, while in the 40% solution the precipitate is flake-like crystallites. The flakes formed with $Al_P$ were completely transparent, and when we tried to examine the structure using SEM (with a probe energy of 20 kEv) at magnification, the sample began to crack. The microstructural surface was smooth, the inhomogeneities present on it represented dislocation defects, and the 1D structures were inside the clefts. In the samples with a solution concentration of 32.6%, 1D structures were nanoscale and did not have hexagons at their base, but rather resembled needles in Figure 6 (**c**).

Figure 7 shows the EDS data, from which the compositions on the surface of sample 5.2 and in the gap are slightly different. The macrostructure of the resulting compound based on food-grade aluminum is in a polycrystalline state. One of the reasons for the presence of crystallites is the level of purity of the laboratory room and local temperature gradients. As noted earlier, the reaction was violent, which is why the phase transitions may have been exothermic in nature. Dislocation transitions are clearly visible. All the resulting samples obtained from both $Al_f$ and $Al_p$ are stoichiometric compounds of $AlF_3$. In the case of $Al_f$, the total impurity is less than 1%.

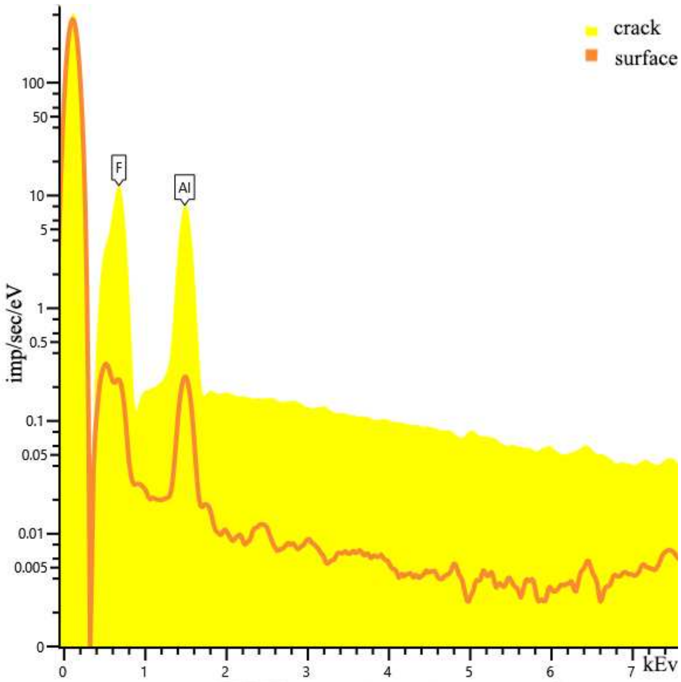


**Figure 7.** EDS data of sample 5.2.

## 4. Conclusions

To sum up, we have demonstrated the possibility of obtaining 1D $AlF_3$ structures under normal conditions. Due to the ease of the production method, these $AlF_3$ NWs can be applied in sensorics, high-performance electronics, and scanning probe microscopy. The obtained stoichiometric Alp-based $AlF_3$ NWs can also be used as a dielectric in supercapacitors due to their predisposition to active charge accumulation. It is known that the use of Alp in the $AlF_3/SiO_2/Si$ system allows one to localize a high density of fixed negative charges in fluorine vacancies, serving as a source of a strong drift field [15]. The robustness of the technological method under normal conditions enables the fabrication of new composite materials based on $AlF_3$, obtaining multilayer structures with 1D nanocrystals with interesting electro-physical properties that can be used for the design of different microelectronic components.

**Author Contributions:** All authors contributed equally, and have read and approved the manuscript.

**Funding:** Research grant of St. Petersburg State University (ID 94033852).

**Data Availability Statement:** Not applicable.

**Acknowledgments:** AD gratefully acknowledges financial support of a research grant of St. Petersburg State University (ID 94033852).

**Conflicts of Interest:** The authors declare no conflict of interest.

## References


1. E. Kemnitz and D. H. Menz, Prog. Solid State Chem., 1998, 26, 97– 153.
2. J. K. Murthy, U. Gross, S. Rudiger, E. Unveren and E. Kemnitz, J. Fluorine Chem., 2004, 125, 937–949.
3. Tang S. et al. Dissolution reaction of TiO2 in molten 6.58 NaF-AlF3: A Raman spectroscopy and computational simulation study //Journal of Molecular Liquids. – 2022. – Т. 367. – С. 120431.
4. Zhou H. et al. Enhanced effect of AlF3 and its Co-regulatory effect with micron-scaled α-Al2O3 nuclei on alumina crystal growth in high-temperature calcination process //Ceramics International. – 2023. – Т. 49. – №. 4. – С. 6563-6572.
5. Zhou H. et al. Enhanced effect of AlF3 and its Co-regulatory effect with micron-scaled α-Al2O3 nuclei on alumina crystal growth in high-temperature calcination process //Ceramics International. – 2023. – Т. 49. – №. 4. – С. 6563-6572.
6. Becker C., Braun T., Paulus B. Theoretical Study on the Lewis Acidity of the Pristine AlF3 and Cl-Doped α-AlF3 Surfaces //Catalysts. – 2021. – Т. 11. – №. 5. – С. 565.
7. M. Kumar and S. S. Sekhon, J. Phys. D: Appl. Phys., 2001, 34, 2995– 3002.
8. S. Fujihara and K. Tokumo, J. Fluorine Chem., 2009, 130, 1106–1110.
9. S. Fujihara, T. Kato and T. Kimura, J. Mater. Sci. Lett., 2001, 20, 687–689.
10. Y. P. Du, Y. W. Zhang, Z. G. Yan, L. D. Sun and C. H. Yan, J. Am. Chem. Soc., 2009, 131, 16364–16365.
11. W. Feng, L. D. Sun, Y. W. Zhang and C. H. Yan, Coord. Chem. Rev., 2010, 254, 1038–1053.
12. Mechanism of oxide film removal by KF-AlF3 and CsF-AlF3 mixed fluxes on Cu and Al base metals and their effect on wettability
13. Al-Assadi Z. I., Sultan M. F. Comparative Study for Designing Two Optical Multilayers Stacks ThF4/AlF3 and ThF4/LiF //Al-Mustansiriyah Journal of Science. – 2022. – Т. 33. – №. 2. – С. 98-102.
14. Gutiérrez-Luna N. et al. Temperature dependence of AlF3 protection on far-UV Al mirrors //Coatings. – 2019. – Т. 9. – №. 7. – С. 428.
15. Praseodymium mid-infrared emission in AlF3-based glass sensitized by ytterbium
16. Li X. et al. Atomic layer deposition of insulating alf3/polyimide nanolaminate films //Coatings. – 2021. – Т. 11. – №. 3. – С. 355.
17. Physical, chemical, and biological properties of white MTA with additions of AlF3
18. Luo Z. et al. AlF3 coating as sulfur immobilizers in cathode material for high performance lithium-sulfur batteries //Journal of Alloys and Compounds. – 2020. – Т. 812. – С. 152132.
19. Lei C. et al. Reduction of porous carbon/Al contact resistance for an electric double-layer capacitor (EDLC) //Electrochimica acta. – 2013. – Т. 92. – С. 183-187.
20. Zhang J. et al. AlF3 coating improves cycle and voltage decay of Li-rich manganese oxides //Journal of Materials Science. – 2023. – Т. 58. – №. 10. – С. 4525-4540.
21. Rodríguez S. J. et al. A theoretical study on the intercalation and diffusion of AlF 3 in graphite: its application in rechargeable batteries //Physical Chemistry Chemical Physics. – 2021. – Т. 23. – №. 35. – С. 19579-19589.
22. Adhitama E. et al. Revealing the Role, Mechanism, and Impact of AlF3 Coatings on the Interphase of Silicon Thin Film Anodes //Advanced Energy Materials. – 2022. – Т. 12. – №. 41. – С. 2201859.
23. Padamata S. K., Yasinskiy A., Polyakov P. Electrode processes in the KF–AlF 3–Al 2 O 3 melt //New Journal of Chemistry. – 2020. – Т. 44. – №. 13. – С. 5152-5164.
24. Abdullayev A. et al. AlF3-assisted flux growth of mullite whiskers and their application in fabrication of porous mullite-alumina monoliths //Open Ceramics. – 2021. – Т. 7. – С. 100145.
25. Estruga M. et al. Large-scale solution synthesis of α-AlF 3· 3H 2 O nanorods under low supersaturation conditions and their conversion to porous β-AlF 3 nanorods //Journal of Materials Chemistry. – 2012. – Т. 22. – №. 39. – С. 20991-20997.
26. Han W. et al. PVDF mediated fabrication of freestanding AlF3 sub-microspheres: Facile and controllable synthesis of α, β and θ-AlF3 //Materials Chemistry and Physics. – 2020. – Т. 240. – С. 122287.
27. Jia W. Z. et al. A novel method for the synthesis of well-crystallized β-AlF3 with high surface area derived from γ-Al2O3 //Journal of Materials Chemistry. – 2011. – Т. 21. – №. 25. – С. 8987-8990.
28. Liu W. et al. 3D spiny AlF3/Mullite heterostructure nanofiber as solid-state polymer electrolyte fillers with enhanced ionic conductivity and improved interfacial compatibility //Journal of Energy Chemistry. – 2023. – Т. 76. – С. 503-515.

 doi:10.20944/preprints202308.0485.v1



29. Mao W. et al. The ethylene glycol-mediated sol–gel synthesis of nano AlF 3: structural and acidic properties after different post treatments //Dalton Transactions. – 2022. – T. 51. – №. 3. – C. 935-945.
30. Deng X. et al. Fabrication and characterization of mullite-whisker-reinforced lightweight porous materials with $AlF_3 \cdot 3H_2O$ //Ceramics International. – 2022. – T. 48. – №. 10. – C. 14891-14898.
31. Kemnitz E. Nanoscale metal fluorides: a new class of heterogeneous catalysts //Catalysis Science & Technology. – 2015. – T. 5. – №. 2. – C. 786-806.
32. Kemnitz E. et al. Amorphous metal fluorides with extraordinary high surface areas //Angewandte Chemie International Edition. – 2003. – T. 42. – №. 35. – C. 4251-4254.
33. Krysztafkiewicz A., Rager B., Maik M. Silica recovery from waste obtained in hydrofluoric acid and aluminum fluoride production from fluosilicic acid //Journal of hazardous materials. – 1996. – T. 48. – №. 1-3. – C. 31-49.
34. Le Bail A. et al. Crystal structure of the metastable form of aluminum trifluoride β-$AlF_3$ and the gallium and indium homologs //Journal of Solid State Chemistry. – 1988. – T. 77. – №. 1. – C. 96-101.
35. König D., Ebest G. Antipolar Counterpart to the Positively Charged $SiO_xN_y$ Layer for Improvement of Field Effect Solar Cells.